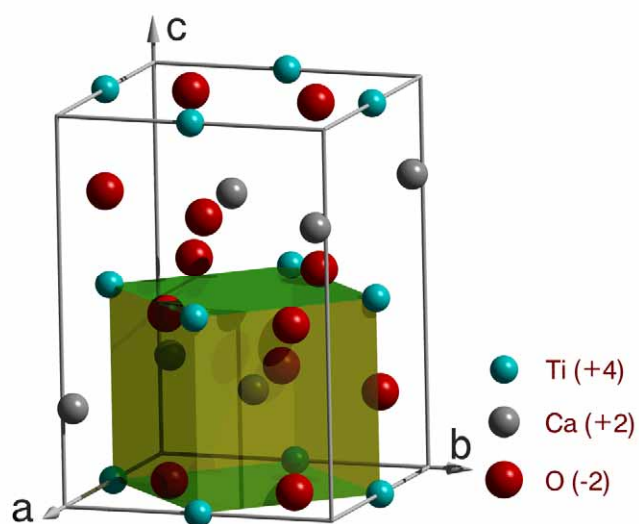


## Supporting Information

# Perovskite Hollow Cubes: Morphological Control, Three-dimensional Twinning and Intensely Enhanced Photoluminescence

*Xianfeng Yang, Ian D. Williams, Jian Chen, Jing Wang, Huifang Xu, Hiromi Konishi, Yuexiao Pan,  
Chaolun Liang and Mingmei Wu\**

\* To whom correspondence should be addressed



**Figure S1:** Schematic structural relationship between the orthorhombic unit cell and the pseudocubic subcell of CaTiO<sub>3</sub>. The green and yellow planes are {002}<sub>o</sub> and {110}<sub>o</sub> lattice planes, respectively. For orthorhombic CaTiO<sub>3</sub> (denoted by subscript o hereafter)  $a_o = 0.5408$ ,  $b_o = 0.5455$  and  $c_o = 0.7678$  nm (JCPDS card No. 82-0229), and for cubic CaTiO<sub>3</sub> (denoted by subscript c)  $a_c = b_c = c_c = 0.3800$  nm (JCPDS card No. 65-3287). Thus, the unit cell of the orthorhombic CaTiO<sub>3</sub> is related to the pseudocubic subcell (subscript pc) by the following relationships:  $a_o \approx b_o \approx \sqrt{2} a_{pc}$  and  $c_o \approx 2a_{pc}$ .

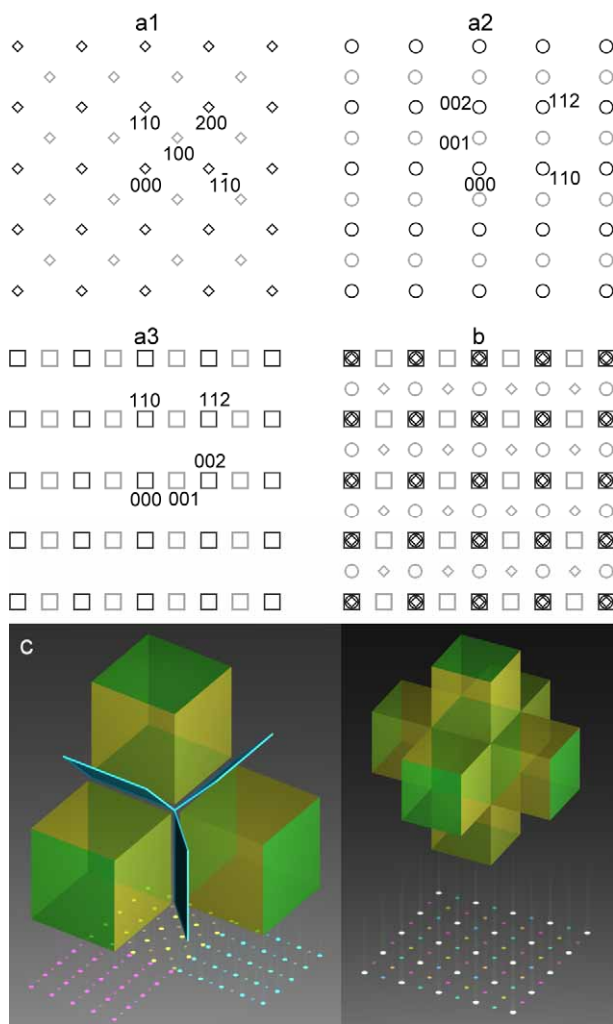


**Figure S2:** (a1-3) Theoretical diffraction patterns viewed along the zone axes of  $[001]_o$ ,  $[1-10]_o$  and  $[-110]_o$ , respectively. Black symbols are the allowed reflections, and gray ones are forbidden reflections. (b) is the combination of (a1-3). (c) Three dimensionally colored views: the left schematic picture illustrates three individual pseudocubic subcells mirrored with each other by the  $\{112\}_o$  [i.e. corresponding to  $\{110\}_{pc}$ ] planes; the yellow, purple and blue diffraction patterns are related to the three sets of diffraction patterns (a1-3), i.e. from the three individual ideal domains, respectively; the right view shows a cross model combined by several pseudocubes, and its corresponding combined diffraction pattern.

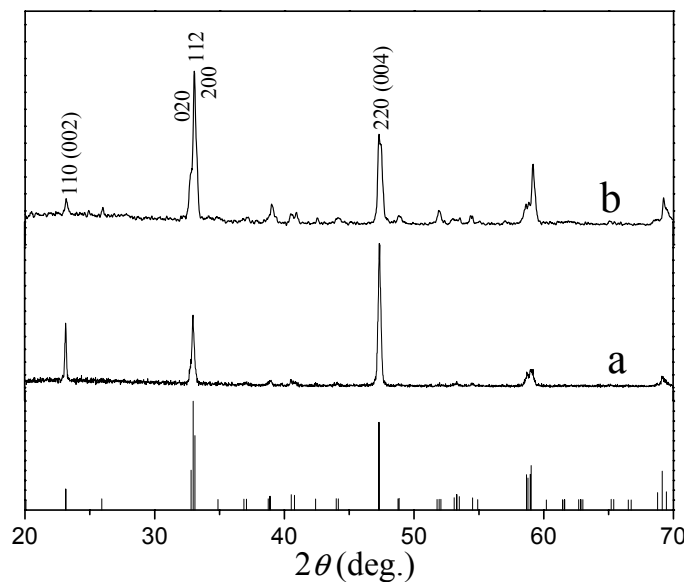


**Figure S3:** Powder XRD patterns of CaTiO<sub>3</sub> products from different media with an increase of water content (a) 10 % (v/v) and (b) 50 % (v/v).

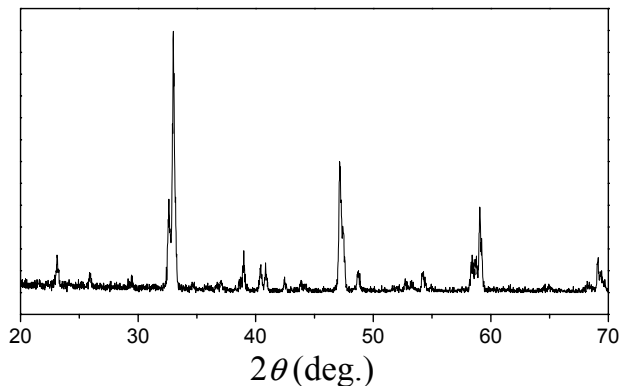
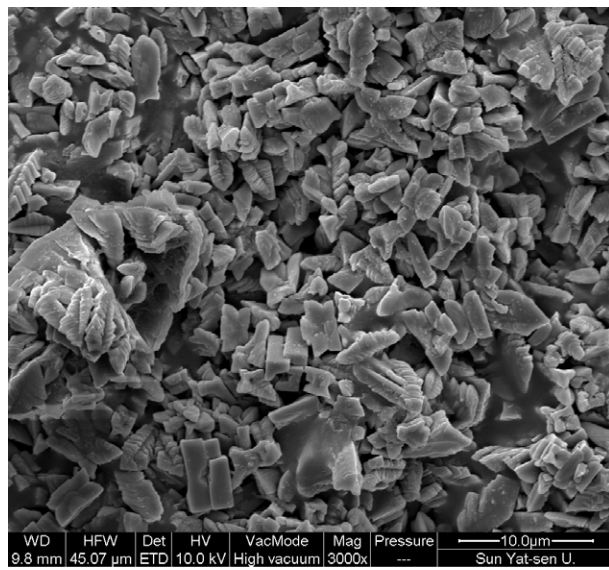


**Figure S4:** SEM image and Powder XRD pattern of hydrothermally produced CaTiO<sub>3</sub> product (i.e. with *pure water* as solvent).

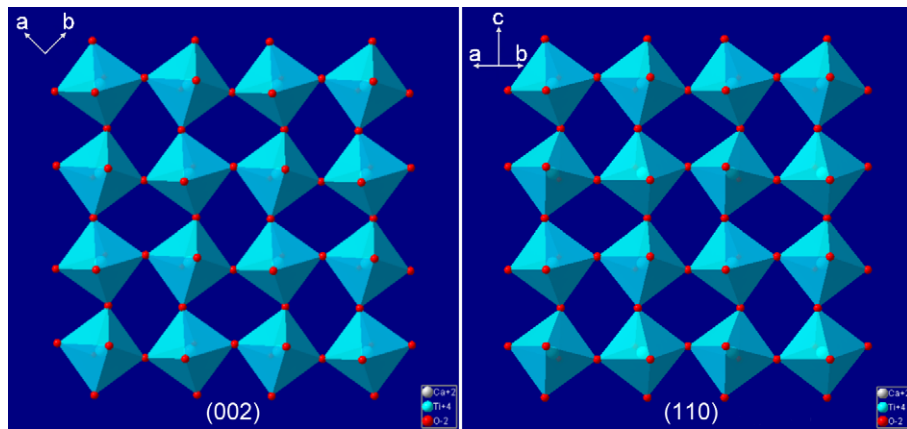


**Figure S5:** The connections of  $\text{TiO}_6$  octahedra on (002) and (110) planes of orthorhombic  $\text{CaTiO}_3$ .

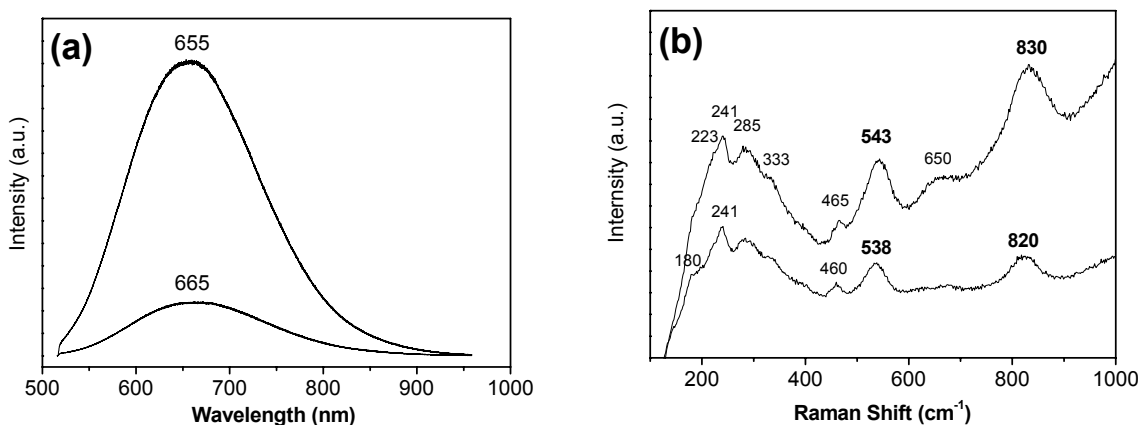


**Figure S6:** a) Photoluminescence and b) Raman spectra of sample 1 (hollow mesocubes) from PEG (upper curve) and sample 2 (rectangular prisms) from mixture of 90%PEG/10%water (lower curve). The intensity of the PL peak at ca. 655 nm from sample 1 is enhanced about six times of that from sample 2 (at ca. 665 nm), indicating the high presence of defects in the twinned-nanodomains-assembled mesoboxes as described in a recently published work.<sup>[1]</sup> The PL position at 665 nm is a greatly red shift from that in the previous work at ca. 600 nm,<sup>[1]</sup> showing its unique PL performance. Figure b shows their Raman spectra. The assignment of these Raman bands at ca. 180, 223, 241, 285, 333, 465, and 650  $\text{cm}^{-1}$  (Fig. S6b) has been well established for bulk **perovskite**  $\text{CaTiO}_3$ .<sup>[2-4]</sup> Two extra bands at about 540 and 825  $\text{cm}^{-1}$  of significant intensity are found, which are not observed in general bulk  $\text{CaTiO}_3$ .<sup>[2-4]</sup> However, they were found in  $\text{CaTiO}_3$ -based **perovskite** solid solutions.<sup>[5-7]</sup> We speculate that the wave-vector selection rules in the present case break down due to the possible presence of  $\text{TiO}_5$  and  $\text{CaO}_{11}$  coordination<sup>[1]</sup> and they become Raman-active in the unique  $\text{CaTiO}_3$  mesoboxes. Raman spectra of orthorhombic  $\text{CaTiO}_3$  crystals were obtained with Renishaw inVia Raman microscope using 514.5 nm excitation laser line under irradiation of 10 %  $\times$  20 mW. The spectra were taken with Leica 50 $\times$  objective, and spectra resolution was 1.0  $\text{cm}^{-1}$ . For PL measurements, using the same laser line of 514.5 nm, the spectrum range was extended to 50-9000 $\text{cm}^{-1}$ , i.e. 515-958 nm. All the spectra were calibrated using the 520.0  $\text{cm}^{-1}$  line of a silicon wafer.

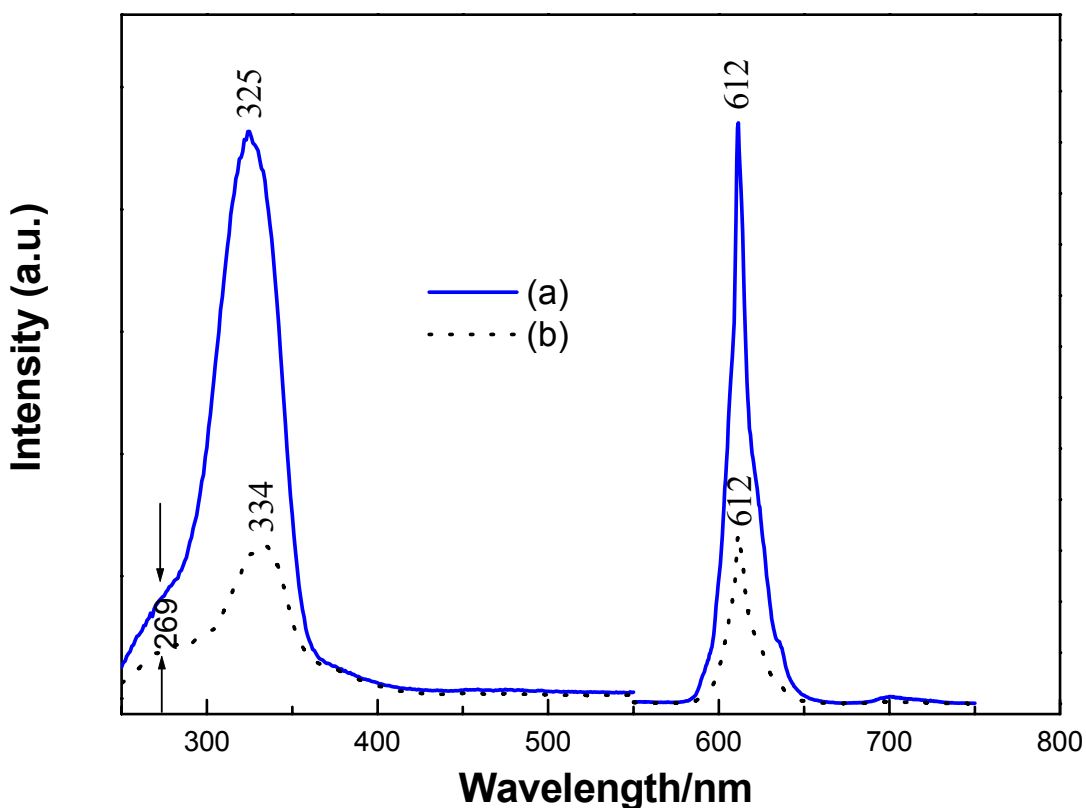


**Figure S7:** Photoluminescence (PL) excitation ( $\lambda_{em}=612$  nm) and emission ( $\lambda_{ex}=325$  nm) spectra of  $\text{CaTiO}_3:\text{Pr}^{3+}$  (0.3%) for sample (a, mesoboxes) and sample (b, prismatic rods).

Under the excitation at 325 nm, the samples show a intense sharp red emission predominating at 612 nm due to the characteristic  $^1\text{D}_2 \rightarrow ^3\text{H}_4$  transition of  $\text{Pr}^{3+}$  in  $\text{CaTiO}_3$ . Monitoring the emission light at 612 nm, there are two broad bands at 269 and 334 nm for sample b, and 269 and 325 nm for sample a. The shoulder band at high-energy side is due to the 4f-5d absorption transition of  $\text{Pr}^{3+}$ .<sup>[8, 9]</sup> The predominating band at low energy side is assigned to the absorption band edge of the  $\text{CaTiO}_3$  host. The blueshift of the host absorption band from 334 nm in sample b to 325 nm in sample a is obviously observed, possibly due to the size confinement effect.<sup>[9]</sup> The most significant observation herein is that the red emission of sample a is much stronger than that of sample b. The integrated PL intensity for the sample a is three times as strong as that of the sample b.

#### Experimental:

The PL excitation and emission spectra at room temperature (RT) were measured on a FLS920-combined Time Resolved and Steady State Fluorescence Spectrometer (Edinburgh Instruments) equipped with a 450W steady-state Xenon lamp.

**References for SI:**

- [1] S. de Lazaro, J. Milanez, A. T. de Figueiredo, V. M. Longo, V. R. Mastelaro, F. S. De Vicente, A. C. Hernandes, J. A. Varela, E. Longo, *Appl. Phys. Lett.*, **2007**, *90*, 111904.
- [2] U. Balachandran, N. G. Eror, *Solid State Commun.*, **1982**, *44*, 815.
- [3] T. Hirata, K. Ishioka, M. Kitajima, *J. Solid State Chem.*, **1996**, *124*, 353.
- [4] S. Qin, X. Wu, F. Seifert, A. I. Becerro, *J. Chem. Soc., Dalton Trans.*, **2002**, 3751.
- [5] H. Zheng, H. Bagshaw, G. D. C. C. de Gyorgyfalva, I. M. Reaney, R. Ubic, J. Yarwood, *J. Appl. Phys.*, **2003**, *94*, 2948.
- [6] V. Železný, E. Cockayne, J. Petzelt, M. F. Limonov, D. E. Usvyat, V. V. Lemanov, A. A. Volkov, *Phys. Rev. B*, **2002**, *66*, 224303.
- [7] I. Levin, E. Cockayne, M. W. Lufaso, J. C. Woicik, J. E. Maslar, *Chem. Mater.*, **2006**, *18*, 854.
- [8] Y. X. Pan, Q. Su, H. F. Xu, T. H. Chen, W. K. Ge, C. L. Yang, M. M. Wu, *J. Solid State Chem.*, **2003**, *174*, 69.
- [9] X. M. Zhang, J. H. Zhang, Z. G. Nie, M. Y. Wang, X. G. Ren, X. J. Wang, *Appl. Phys. Lett.*, **2007**, *90*, 151911.